

Alkali Metal Cation Control of Oxidation Reactions of Radicals in Zeolites

Frances L. Cozens,^{*,†} Maria Luz Cano,^{†,§} Hermenegildo García,[‡] and Norman P. Schepp[†]

Contribution from the Department of Chemistry, Dalhousie University, Halifax, Nova Scotia, Canada B3H 4J3, and Instituto de Tecnología Química UPV-CSIC, Universidad Politécnica de Valencia, Apartado 22012, 46071 Valencia, Spain

Received May 12, 1997. Revised Manuscript Received April 6, 1998

Abstract: The dynamics of the xanthyl radical in a series of alkali-metal cation exchanged (Li^+ , Na^+ , K^+ , Rb^+ , and Cs^+) Y faujasites in the absence and presence of molecular oxygen are examined by using laser flash photolysis. Upon laser photolysis of xanthene-9-carboxylate incorporated within the supercages of NaY in the absence of oxygen, prompt formation of the xanthyl radical and the xanthylum cation is observed. The xanthyl radical is formed by photoionization of xanthene-9-carboxylate to the corresponding acyloxy radical that then rapidly decarboxylates. The prompt xanthylum cation is produced by photoionization of the xanthyl radical. This mechanism for the prompt xanthylum cation is supported by results from two-color laser and photoinduced electron transfer experiments. When oxygen is introduced into the sample, the radical is almost completely quenched. In addition, a slow growth of the xanthylum cation at 375 nm is observed. This growth is due to heterolytic cleavage of the peroxy radical formed upon reaction of the xanthyl radical with molecular oxygen. The formation and resulting growth of the xanthylum cation in the presence of oxygen is found to be highly dependent on the zeolite counterion with significant carbocation formation occurring in both LiY and NaY, little carbocation formation in KY, and no carbocation formation in RbY and CsY. These are the first results showing how the oxidation of radicals to carbocations within zeolites can be controlled by simple alkali metal exchange.

Introduction

Zeolites are microporous crystalline aluminosilicate materials made up of $[\text{SiO}_4]^{4-}$ and $[\text{AlO}_4]^{5-}$ tetrahedra arranged in an array of molecular sized pores, channels, and cavities.^{1–3} The open framework construction allows zeolites to act as hosts for a wide range of organic compounds with the appropriate size and shape, and these materials are increasingly being used as constrained media for manipulating photochemical and thermal transformations.^{4–25} Included within the open topology are

metal cations or protons required to balance the net negative charge caused by the presence of each aluminum atom. The nature of the charge-balancing cations can have a dramatic influence on the effect of zeolites on chemical reactions of included organic materials. For example, one of the most important applications of zeolites is the acid-catalyzed hydrocarbon cracking processes used in the petroleum industry.²⁶ For this application, the charge balancing cations are typically protons, which give the zeolite remarkably powerful proton-donating and electron-accepting abilities required to catalyze carbocation or

[†] Dalhousie University.

[§] On leave from the Instituto de Tecnología Química UPV-CSIC.

[‡] Universidad Politécnica de Valencia.

(1) *Introduction to Zeolite Science and Practice*; van Bekkum, H., Flanigen, E. M., Jansen, J. C., Eds.; Elsevier: Amsterdam, 1991.

(2) Dyer, A. *An Introduction to Zeolite Molecular Sieves*; John Wiley & Sons: Bath, U.K., 1988.

(3) Barrer, R. M. *Zeolites and Clay Minerals as Sorbents and Molecular Sieves*; Academic Press: London, 1978.

(4) Alvaro, M.; García, H.; Carcía, S.; Marquez, F.; Scaiano, J. C. *J. Phys. Chem. B* **1997**, *101*, 3043–3051.

(5) Baldoví, M. V.; Cozens, F. L.; Fornés, V.; García, H.; Scaiano, J. C. *Chem. Mater.* **1996**, *8*, 152–160.

(6) Cano, M. L.; Fornés, V.; García, H.; Miranda, M. A.; Pérez-Prieto, J. *J. Chem. Soc., Chem. Commun.* **1995**, 2477–2478.

(7) Cano, M. L.; Corma, A.; Fornés, V.; García, H. *J. Phys. Chem.* **1995**, *99*, 4241–4246.

(8) Cano, M. L.; Cozens, F. L.; Vicente, F.; García, H.; Scaiano, J. C. *J. Phys. Chem.* **1996**, *100*, 18145–18151.

(9) Cano, M. L.; Cozens, F. L.; García, H.; Vicente, M.; Scaiano, J. C. *J. Phys. Chem.* **1996**, *100*, 18152–18157.

(10) Corma, A.; Fornés, V.; García, H.; Martí, V.; Miranda, M. A. *Chem. Mater.* **1995**, *7*, 2136–2143.

(11) Corma, A.; Fornés, V.; García, H.; Miranda, M. A.; Primo, J.; Sabater, M. *J. Am. Chem. Soc.* **1994**, *116*, 2276–2280.

(12) Cozens, F. L.; García, H.; Scaiano, J. C. *Langmuir* **1994**, *10*, 2246–2249.

(13) Cozens, F. L.; Régimbald, M.; García, H.; Scaiano, J. C. *J. Phys. Chem.* **1996**, *100*, 18165–18172.

(14) Cozens, F. L.; García, H.; Scaiano, J. C. *J. Am. Chem. Soc.* **1993**, *115*, 11134–11140.

(15) Cozens, F. L.; O'Neill, M.; Schepp, N. P. *J. Am. Chem. Soc.* **1997**, *119*, 7583–7584.

(16) Ramamurthy, V.; Caspar, J. V.; Corbin, D. R.; Schlyer, B. D.; Maki, A. H. *J. Phys. Chem.* **1990**, *94*, 3391–3393.

(17) Ramamurthy, V.; Caspar, J. V.; Corbin, D. R. *J. Am. Chem. Soc.* **1991**, *113*, 594–600.

(18) Ramamurthy, V. *Chimia* **1992**, *46*, 359–376.

(19) Pitchumani, K.; Corbin, D. R.; Ramamurthy, V. *J. Am. Chem. Soc.* **1996**, *118*, 8152–8153.

(20) Pitchumani, K.; Lakshminarasimhan, P. H.; Turner, G.; Bakker, M. G.; Ramamurthy, V. *Tetrahedron Lett.* **1997**, *38*, 371–374.

(21) Pitchumani, K.; Lakshminarasimhan, P. H.; Prevost, N.; Corbin, D. R.; Ramamurthy, V. *J. Chem. Soc., Chem. Commun.* **1997**, 181–182.

(22) Xu, T.; Zhang, J.; Munson, E. J.; Haw, J. F. *J. Chem. Soc., Chem. Commun.* **1994**, 2733–2735.

(23) Xu, T.; Haw, J. F. *J. Am. Chem. Soc.* **1994**, *116*, 7753–7759.

(24) Xu, T.; Haw, J. F. *J. Am. Chem. Soc.* **1994**, *116*, 10188–10195.

(25) Yoon, K. B.; Kochi, J. K. *J. Am. Chem. Soc.* **1988**, *110*, 6586–6588.

(26) Jacobs, P. A.; Martens, J. A. In *Introduction to Zeolite Science and Practice*; van Bekkum, H., Flanigen, E. M., Jansen, J. C., Eds.; Elsevier: Amsterdam, 1991; Vol. 58, pp 445–496.

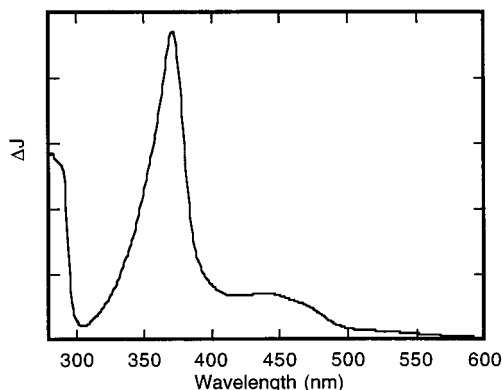


Figure 1. Steady-state diffuse reflectance spectrum of xanthene-9-carboxylic acid in HY.

radical cation formation for the cracking reactions.²⁷ Other cation exchanged zeolites have catalytic properties that differ from proton-exchanged zeolites. Thus, introduction of Ca^{2+} results in the formation of Brønsted acid sites that are considerably weaker than the Brønsted acid strength of proton exchanged zeolites, but considerably stronger than the acid strength of alkali-metal exchanged zeolites.²¹

The ability to modify the catalytic role played by the zeolite simply by introducing different metal cations indicates that zeolites may be used as selective catalysts for the preparation of a wide range of organic compounds. With this in mind, it would be useful to have the ability to predict how changing zeolite composition affects the course of fundamental reactions in organic chemistry. One method by which to provide information that can be used to help make these kinds of predictions in a rational manner is to examine the effect of zeolite composition on the dynamics and mechanisms of reactions taking place within the zeolite cavities. In the present work, we describe our results from a nanosecond diffuse reflectance study of the oxidation of the xanthyl radical to the xanthylum cation in alkali-metal cation exchanged zeolites. Our results show that the alkali metal cation exchanged zeolites are not sufficiently strong oxidizing agents to convert the xanthyl radical to the xanthylum cation, but that oxidation to the carbocation within the zeolite cavities can be induced by the addition of molecular oxygen. More importantly, the oxidation is strongly influenced by the nature of the counterion. Thus, in the Li^+ and Na^+ exchanged zeolites, the radical is efficiently converted to the carbocation in the presence of oxygen, while in Rb^+ and Cs^+ exchanged samples, little or no oxygen-induced carbocation formation is observed. These results therefore demonstrate that counterions can be used to adjust the chemoselectivity of radical reactions taking place within the cavities of zeolites.

Results

Characterization of XCOOH/Zeolite Composites. Xanthene-9-carboxylic acid (XCOOH) is readily incorporated into each of the metal cation exchanged zeolites, LiY, NaY, KY, RbY, and CsY, used in the present work. No color formation was observed upon incorporation of XCOOH into each of the alkali exchanged Y zeolites, and only XCOOH was recovered from the zeolites upon continuous solid-liquid extraction, indicating that XCOOH is thermally stable within the zeolites for several days. The one exception was incorporation of XCOOH into the acidic zeolite, HY, which resulted in rapid formation of a bright yellow color. The diffuse reflectance

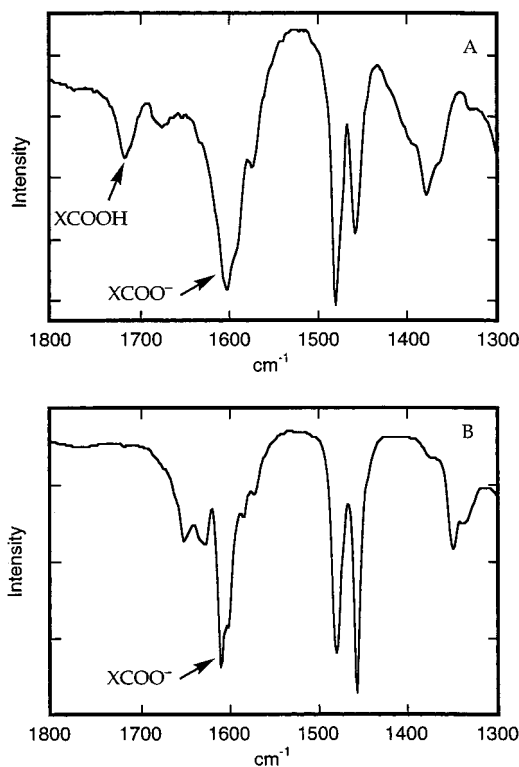
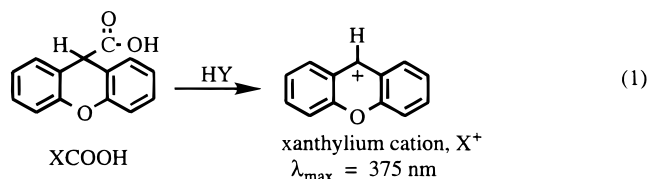


Figure 2. IR spectra of xanthene-9-carboxylic acid incorporated within NaY (A) and CsY (B).

spectrum shown in Figure 1 clearly shows a maximum at 375 nm that corresponds closely to the maximum of the xanthylum cation, X^+ , in acidic solution,^{28,29} indicating that XCOOH spontaneously decomposes to give X^+ upon incorporation into HY, eq 1.



In the nonprotic cation exchanged zeolites, IR spectra were obtained to determine if XCOOH exists to a significant extent as the carboxylate ion, XCOO^- . The spectra obtained in NaY and CsY are shown in Figure 2. In NaY, a carbonyl stretching band at 1717 cm^{-1} assigned to XCOOH is observed, but it is accompanied by a stronger band at 1611 cm^{-1} , which is consistent with the presence of the carboxylate ion, XCOO^- . In CsY, only the band at 1611 cm^{-1} is observed, which would be expected due to the higher Brønsted basicity of CsY compared to NaY.^{4,30–32} These results therefore indicate that the ionized form of the acid is the dominant form in the alkali-metal exchanged zeolites.

Diffuse Reflectance Spectra under Vacuum Conditions in MY.

The diffuse reflectance spectrum generated upon 266-

(28) McClelland, R. A.; Banait, N.; Steenken, S. *J. Am. Chem. Soc.* **1989**, *111*, 2929–2935.

(29) Clifton, M. F.; Fenick, D. J.; Gasper, S. M.; Falvey, D. E.; Boyd, M. K. *J. Org. Chem.* **1994**, *59*, 8023–8029.

(30) Corma, A.; Fornés, V.; Martín-Aranda, R. M.; García, H.; Primo, J. *Appl. Catal.* **1990**, *59*, 237–248.

(31) Lavalley, J.; Lamotte, J.; Travert, A.; Czyżniewska, J.; Ziolk, M. *J. Chem. Soc., Faraday Trans.* **1998**, *94*, 331–335.

(32) Liu, X.; Iu, K.; Thomas, J. K. *J. Phys. Chem.* **1994**, *98*, 7877–7884.

(27) Corma, A. *Chem. Rev.* **1995**, *95*, 559–614.

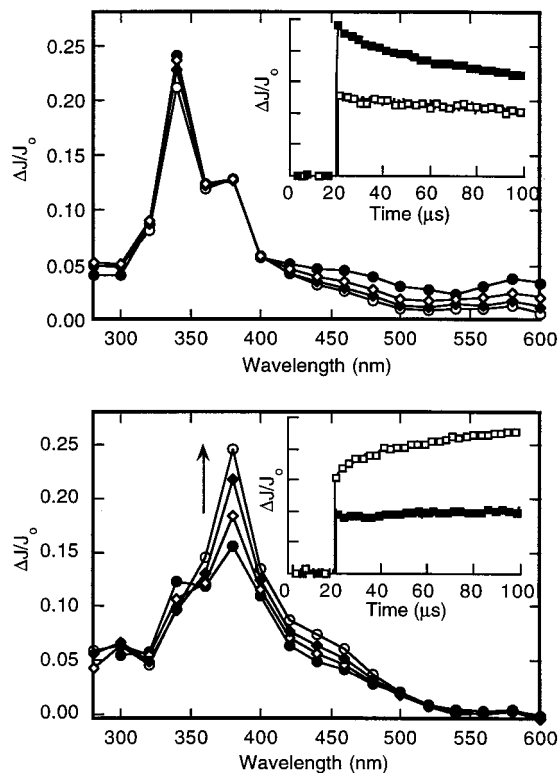
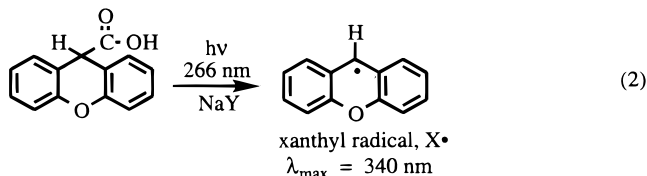


Figure 3. Transient reflectance spectrum generated upon 266 nm laser photolysis of xanthene-9-carboxylic acid in dry, evacuated (10^{-3} Torr) NaY (top) and in dry, oxygen-purged NaY (bottom). Spectra were recorded (●) 0.36, (◇) 1.04, (◆) 3.32, and (○) 11.8 μ s after the laser pulse. The insets show the time-resolved kinetics at (■) 340 and (□) 375 nm over 100 μ s.

nm laser irradiation of XCOOH in dry NaY under vacuum (10^{-3} Torr) conditions is shown in Figure 3 (top). The spectrum shows that laser photolysis results in the formation of a transient species with an absorption maximum at 340 nm. This species is quite long-lived, with only about 30% of the absorption decaying within 80 μ s after the laser pulse. When the kinetic trace is taken over a 500 μ s time scale, the decay of the 340-nm band can be adequately fit to a double first-order expression to give a fast and slow component with decay rate constants of 2.8×10^4 and 1.8×10^3 s^{-1} , respectively. The location of the absorption band at 340 nm is identical to that for the maximum of the xanthyl radical previously generated in solution.^{29,33,34} In addition, the band at 340 nm is completely quenched by the addition of molecular oxygen to the dry NaY zeolite (vide infra). On the basis of these observations, the transient produced from XCOOH upon 266-nm laser excitation can be confidently identified as the xanthyl radical, X^{\bullet} , eq 2.



Similar results were observed upon laser photolysis of XCOOH incorporated into the other dry cation exchanged zeolites, LiY, KY, RbY, and CsY, under vacuum (10^{-3} Torr) conditions. In each case, the dominant feature of the time-resolved diffuse

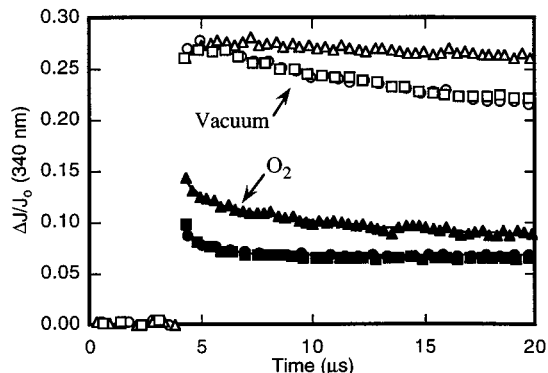


Figure 4. Decay of the xanthyl radical at 340 nm generated by 266-nm laser irradiation of xanthene-9-carboxylic acid in evacuated (10^{-3} Torr) LiY (○), NaY (□), and CsY (△), and in oxygen-saturated LiY (●), NaY (■), and CsY (▲).

reflectance spectrum was a strong absorption band at 340 nm due to the formation of X^{\bullet} upon laser irradiation.

As shown in Figure 3 (top), a second transient species with a maximum at 375 nm is also observed immediately upon laser irradiation of XCOOH in NaY. Unlike X^{\bullet} at 340 nm, the band at 375 nm shows almost no decay over time periods as long as 100 μ s, indicating that the absorption at 375 nm is not due to the presence of X^{\bullet} . We assign this band to the xanthylum cation, X^+ , which is known to have an absorption maximum at approximately the same location in HY (Figure 1) and in solution.^{12,28,29} Prompt formation of X^+ at 375 nm was also observed in the other cation exchanged zeolites upon photolysis of XCOOH. In each case, the ratio of the intensity of the band at 340 nm due to the presence of X^{\bullet} to that at 375 nm due to the presence of X^+ remained constant at about 2:1.

Diffuse Reflectance Spectra under O_2 Conditions in MY.

Classic evidence for assignment of a transient species as a radical is the observation of oxygen quenching.¹⁴ As can be seen in Figure 3 (bottom), the intensity of the 340-nm band immediately after the laser pulse is dramatically reduced upon the addition of oxygen to the NaY sample. The 340-nm band is not completely quenched, Figure 4, but the remaining absorption decays rapidly with a rate constant of about 1.0×10^6 s^{-1} that is considerably greater than the rate constant under vacuum conditions. Both observations support our identification of the 340-nm transient as the xanthyl radical, X^{\bullet} .³⁵

The large reduction in the intensity of the radical signal immediately after the laser pulse in the cation exchanged zeolites is consistent with oxygen rapidly quenching >85% of the radicals produced upon laser irradiation. The fact that this quenching is too fast to be resolved indicates that the majority of the xanthyl radicals decay with a rate constant $>10^7$ s^{-1} in the presence of oxygen. The subsequent slower decay of the remaining ~15% of the radicals is presumably due to xanthyl radicals residing in less accessible environments within the zeolite framework.¹⁴ It should be noted that the quenching effect of oxygen is similar in all of the cation exchanged Y zeolites, although in CsY quenching of the radical was slightly inhibited by the large cation size.

More interestingly, the presence of oxygen within the NaY zeolite also induces the time-resolved formation of a transient species that can be identified as the xanthylum cation on the basis of its absorption spectrum and maximum, $\lambda_{\text{max}} = 375$ nm, Figure 3 (bottom). Under these conditions, a strong growth at 375 nm due to the formation of X^+ is observed over a time

(33) Samanta, A.; Gopidas, K. P.; Das, P. K. *J. Phys. Chem.* **1993**, *97*, 1583–1588.

(34) Minto, R. E.; Das, P. K. *J. Am. Chem. Soc.* **1989**, *111*, 8858–8866.

(35) The quenching of radicals in zeolites generally does not lead to the complete disappearance of the radical absorption.

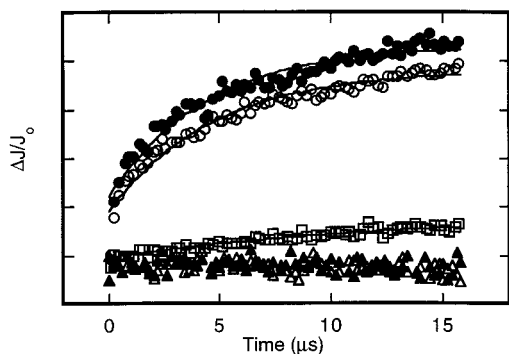
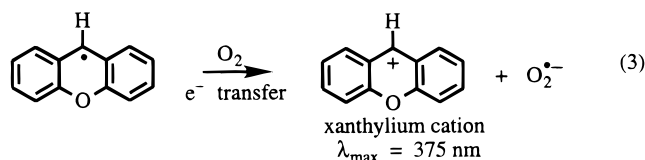


Figure 5. Change in diffuse reflectance at 375 nm as a function of time upon 266-nm laser irradiation of xanthene-9-carboxylic acid in oxygen-purged LiY (●), NaY (○), KY (□), RbY (△), and CsY (▲).

period of $>100 \mu\text{s}$. The fact that this growth is only observed in the presence of oxygen provides firm evidence that it is the radical that is being oxidized by molecular oxygen to generate X^+ by a formal one-electron-transfer mechanism, eq 3.²⁹



The time-resolved changes in diffuse reflectance at 375 nm due to the formation of the xanthylum cation in the various oxygen-purged alkali exchanged zeolites, Figure 5, illustrate that the xanthylum cation is produced upon photolysis of XCOOH in LiY and NaY and to a lesser extent in KY. The traces in Figure 5 also show that carbocation formation does not take place upon quenching of X^{\bullet} by oxygen in either RbY or CsY. Thus, despite the fact that the radical is quenched rapidly in much the same manner in RbY and CsY as it is in LiY and NaY, quenching of the radicals in the zeolites containing the larger alkali metal cations does not lead to carbocation formation as observed in LiY and NaY. The growths for X^+ fit reasonably well to a first-order expression that gives a rate constant of ca. $2.1 \times 10^5 \text{ s}^{-1}$ in both LiY and NaY. In KY, an intermediate situation is observed where a small amount of carbocation grows in with a slow first-order rate constant of $\sim 7 \times 10^4 \text{ s}^{-1}$. Thus, the charge-balancing cations have a significant effect on both the yield and the kinetics of the growth of X^+ produced upon oxygen quenching of the xanthyl radical.

Selective formation of X^+ under oxygen conditions can also be observed upon steady-state irradiation. Thus, a XCOOH/NaY composite under vacuum conditions becomes only slightly yellow when irradiated with 254-nm light for 1 h, indicating that little X^+ is generated. However, in the presence of oxygen, 254-nm irradiation for the same time period of 1 h causes the composite to become highly yellow, and diffuse reflectance spectroscopy indicates that irradiation leads to the formation of X^+ in a substantial yield with an absorption maximum at 375 nm. The sample remained yellow for long periods of time (greater than 1 week) if the sample was kept under dry conditions. However, if water is allowed to enter into the zeolite by exposing the sample to the air the yellow color disappears presumably due to quenching of the carbocation by the co-absorption of water.³⁶ In CsY, little yellow color is produced under either vacuum or oxygen conditions upon 254-nm irradiation.

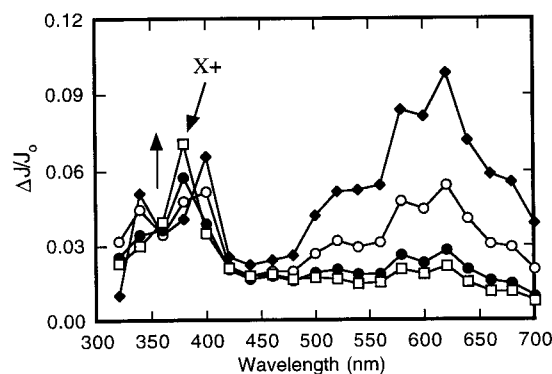
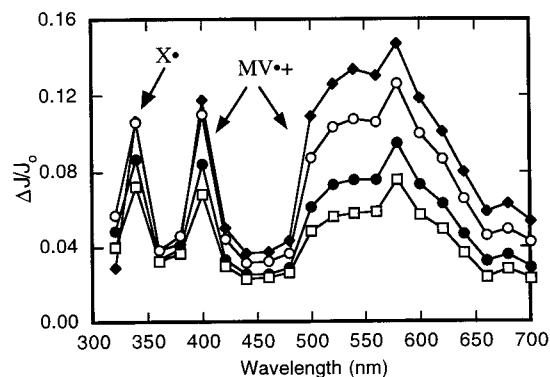


Figure 6. Diffuse reflectance upon 308 nm laser irradiation of methyl viologen and xanthene-9-carboxylic acid incorporated into NaY under vacuum (top) and oxygen-saturated (bottom) conditions. Spectra were recorded (◆) 0.36, (○) 1.04, (●) 3.32, and (□) 11.8 μs after the laser pulse.

Diffuse Reflectance Spectra under Photoinduced Electron-Transfer Conditions. Similar results to those described above from direct laser irradiation were also obtained under photoinduced electron-transfer conditions. In this case, XCOOH was co-incorporated in NaY with methyl viologen dication, MV^{2+} . Selective irradiation of MV^{2+} with 308-nm laser light under vacuum (10^{-3} Torr) conditions resulted in the rapid formation of X^{\bullet} at 340 nm, together with bands at 400 and 600 nm due to the presence of the methyl viologen radical cation,^{4,37} $MV^{\bullet+}$, Figure 6. No absorption at 375 nm due to prompt X^+ is observed under these conditions. X^{\bullet} is long-lived under vacuum conditions, but is rapidly quenched by the addition of oxygen in the same manner as quenching of the radical produced by direct laser irradiation. In addition, under oxygen, after the radical decay is almost complete, a distinct growth at 375 nm due to the formation of X^+ is readily observed, Figure 6.

Diffuse Reflectance Spectra under Two-Color Excitation. Figure 7 shows the results obtained with XCOOH incorporated within RbY under vacuum (10^{-3} Torr) conditions upon two-color excitation.^{38,39} During this experiment the XCOOH/RbY composite is initially excited with 266-nm excitation and then, after a 7- μs delay, the sample is exposed to a 308-nm laser pulse. The starting XCOOH does not appreciably absorb at 308 nm. In fact, only the photogenerated X^{\bullet} absorbs strongly at the 308-nm wavelength of the second laser pulse. As described earlier, both X^{\bullet} and X^+ are formed upon 266-nm excitation, Figure 7. Upon 308-nm excitation 7 μs after the first pulse, bleaching is observed at 340 nm due to consumption

(37) Bockman, T. M.; Hubig, S. M.; Kochi, J. K. *J. Am. Chem. Soc.* **1996**, *118*, 4502–4503.

(38) Faria, J. L.; Steenken, S. *J. Phys. Chem.* **1993**, *97*, 1924–1930.

(39) Faria, J. L.; Steenken, S. *J. Am. Chem. Soc.* **1990**, *112*, 1277–1279.

(36) Cozens, F. L.; Gessner, F.; Scaiano, J. C. *Langmuir* **1993**, *9*, 874–876.

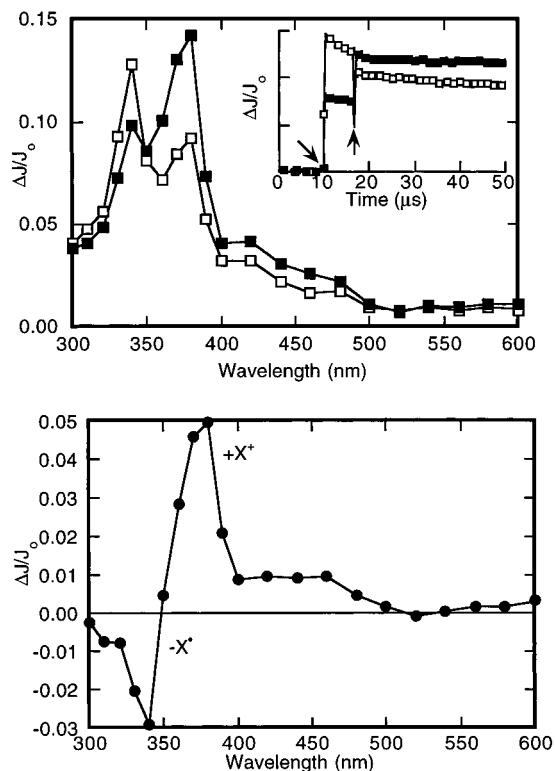
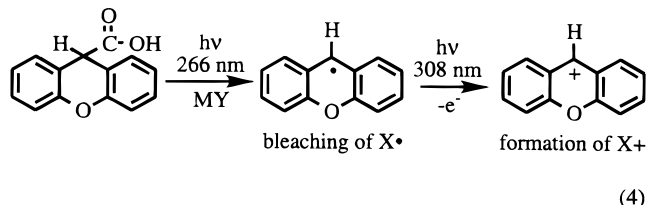


Figure 7. Diffuse reflectance spectrum generated upon two-color excitation, using 266- (□) and 308-nm (■) excitation (top) and the difference spectra showing the effect of 308 nm laser excitation (bottom) of xanthene-9-carboxylic acid incorporated into RbY under vacuum conditions. The inset shows the time-resolved kinetics at (□) 340 and (■) 375 nm.

of X^{\bullet} , and a large increase at 375 nm is observed due to the formation of X^+ , eq 4.



Similar results were obtained in the other cation exchanged zeolites where the radical at 340 nm was bleached upon 308-nm excitation and the carbocation at 375 nm was formed. These results clearly indicate that X^{\bullet} is readily photoionized to X^+ upon laser excitation within the ionizing environment of the zeolite.

Discussion

Effect of Counterion on Oxidation of Radicals. The most important observation in the present work is that oxidation of the xanthyl radical within the Y zeolites to the xanthylum cation can be controlled by the identity of the counterion. Thus, in the presence of molecular oxygen, X^{\bullet} is converted to X^+ when the counterion is Li^+ , or Na^+ , and to a small degree with K^+ , but no radical to carbocation formation takes place when the counterion is Rb^+ or Cs^+ . This indicates clearly that simple alkali metal cation exchange plays a critical role in *determining the chemoselectivity of reactions of radicals in zeolites.*

Close examination of the X^{\bullet} decay and the X^+ growth in LiY and NaY provides some insight into the possible role of

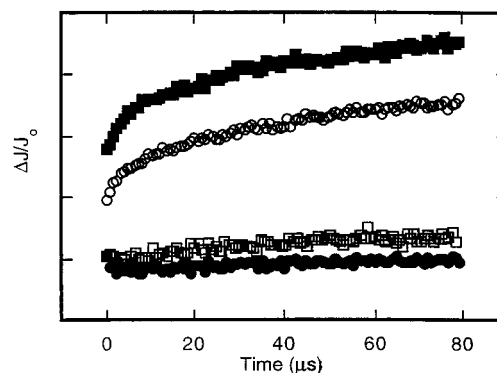
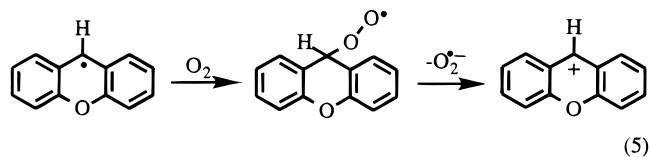


Figure 8. Time-resolved diffuse reflectance changes over 100 μs after 266-nm laser irradiation of xanthene-9-carboxylic acid in oxygen-purged dry NaY at (●) 340 and (○) 375 nm and LiY at (□) 340 and (■) 375 nm.

the cations in controlling the mechanism of radical oxidation and carbocation formation. As shown in Figure 8, in the presence of molecular oxygen the xanthylum cation at 375 nm continues to grow-in long after the radical decay at 340 nm is completely finished. In fact, our results clearly show that while the reaction of the radical with oxygen is complete about 5 μs after the laser pulse, the xanthylum cation at 375 nm continues to be produced, even at times as long as 80 μs after the laser pulse. This behavior whereby X^+ continues to grow after the radical has completely decayed indicates that conversion of the radical to the carbocation involves the presence of an intermediate. In the present case, the most likely intermediate is a peroxy radical produced by addition of molecular oxygen to the radical center, eq 5. Heterolytic cleavage of the C–O bond then leads to the formation of the xanthylum cation and superoxide ion.⁴⁰



Since the counterion has little effect on the first step of the reaction where the radical is consumed by oxygen, we believe that the effect of the charge-balancing cations on the oxidation of the radical to the carbocation most likely takes place during loss of $O_2^{\bullet-}$. Since ESR studies have shown that $O_2^{\bullet-}$ interacts with intracavity cations^{41,42} and this interaction is affected by the nature of the cation,^{43,44} loss of $O_2^{\bullet-}$ may be aided by the smaller cations such as Li^+ or Na^+ that interact more strongly with and therefore provide more stabilization to the $O_2^{\bullet-}$ than the larger cations such as Rb^+ and Cs^+ . In essence, the smaller cations may increase the leaving group ability of the $O_2^{\bullet-}$ anion by stronger electrostatic interactions. The observed effect of the counterion also reflects an increased thermodynamic driving force for radical-to-ion conversion ($X-O-O^{\bullet}$ to $O_2^{\bullet-}$ and X^+) with increasing electrostatic field in the vicinity of the alkali ions in the direction of Li^+ to Cs^+ .⁴⁵

Mechanism of Radical Formation. While the results indicate that laser irradiation of the xanthene-9-carboxylic acid

(40) Such a mechanism has been suggested for oxidation of the xanthyl radical to the xanthylum cation in acidic aqueous solution.²⁹

(41) Imai, T.; Habgood, H. W. *J. Phys. Chem.* **1973**, *77*, 925–931.

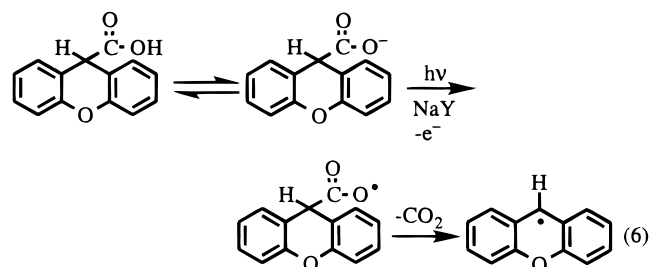
(42) Lunsford, J. H. *Catal. Rev.* **1973**, *8*, 135–157.

(43) Wang, K. M.; Lunsford, J. H. *J. Phys. Chem.* **1970**, *74*, 1512–1517.

(44) Chamulitrat, W.; Kevan, L. *J. Phys. Chem.* **1985**, *89*, 4989–4993.

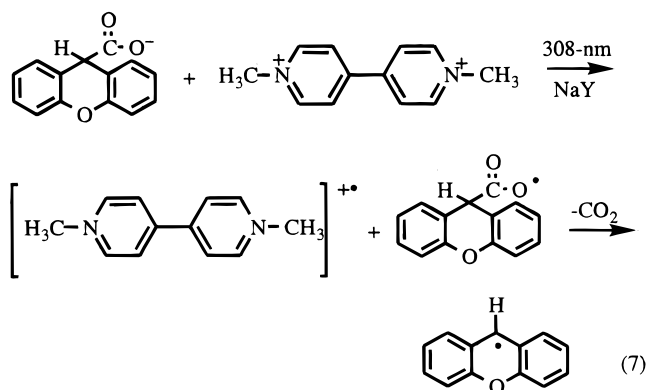
(45) Ramamurthy, V.; Eaton, D. F.; Caspar, J. V. *Acc. Chem. Res.* **1992**, *25*, 299–307.

leads to the formation of X^* , the mechanism for this conversion is not immediately apparent. One possible mechanism is shown in eq 6. According to this equation, the ionized form of the acid is photoionized to the acyloxyl radical, which then undergoes rapid decarboxylation to give the xanthyl radical, eq 6.^{46,47}



Some evidence for this mechanism comes from the IR spectra of xanthene-9-carboxylic acid in NaY and CsY shown in Figure 1. Both spectra indicate that the dominant form of the carboxylic acid is actually the ionized carboxylate ion, as required by the mechanism for radical formation indicated above.

The results with methyl viologen dication as an electron-transfer sensitizer are also consistent with the mechanism shown above. In particular, the observation that selective irradiation of MV^{2+} in the presence of the xanthene-9-carboxylate leads to the formation of the $MV^{\bullet+}$ together with X^* indicates that xanthyl radical formation involves an electron-transfer step, eq 7.



Thus, electron transfer from the carboxylate ion to excited methyl viologen leads to the rapid formation of the methyl viologen radical cation and the acyloxyl radical, which then rapidly decarboxylates to give the xanthyl radical.³⁷

Prompt Cation Formation. In all the alkali metal cation exchanged Y samples examined in the present work, a significant amount of X^+ was formed within the duration of the 8-ns 266-nm laser pulse even when the sample was sealed under vacuum (10^{-3} Torr). Typically, the top reflectance of X^* at 340 nm was approximately twice as strong as the top reflectance of X^+ at 375 nm, Figure 3. The only example where no prompt carbocation formation was observed occurred when the photolysis was carried out with methyl viologen as an electron transfer photosensitizer. In this case, the xanthyl radical was the only product of the electron-transfer reaction under vacuum

(46) Bockman, M. T.; Hubig, S. M.; Kochi, J. K. *J. Org. Chem.* **1997**, *62*, 2210–2221.

(47) Photodecarboxylation to give the xanthyl anion followed by thermal oxidation within the zeolite framework would also lead to xanthyl radical formation.

(10^{-3} Torr) conditions. Since no carbocation was observed under sensitizer conditions, it is unlikely that prompt X^+ formation involves a rapid thermal electron transfer from X^* to the zeolite framework.^{10,19–21,48} Instead, prompt carbocation formation is likely caused by a biphotonic process in which the xanthyl radical is first produced by a fast photoionization/decarboxylation reaction, and then photoionized by a second photon of light from the same laser pulse to yield prompt X^+ . Such two-photon processes are common within zeolites, and photoionization of radicals to carbocations in solution has been observed previously.^{38,39}

Further evidence that prompt carbocation formation involves photoionization of the initially formed X^* comes from the results of the two-color laser experiments. Upon 308-nm excitation of X^* in MY, approximately 25% of the radical signal is bleached, giving rise to the formation of X^+ . The substantial bleaching demonstrates that the radical in the Y zeolites is quite efficiently photoionized to X^+ . If we assume that 100% of the photobleached radicals are photoionized to the carbocation we can estimate that the extinction coefficient of the carbocation is around twice that of the radical,⁴⁹ Figure 7. Upon direct 266-nm irradiation, the magnitude of the top reflectance due to X^* compared to X^+ is typically about 2:1, which indicates that approximately 20% of the initially generated radicals are photoionized to the carbocation within the 266-nm laser pulse. This estimate is similar to the 25% photobleaching observed upon two-color excitation and is consistent with our conclusion that prompt X^+ formation is due to a two-photon ionization reaction.

Conclusion

Irradiation of xanthene-9-carboxylate in alkali metal cation exchanged zeolites under vacuum conditions leads to prompt formation of the xanthyl radical by photoionization/decarboxylation, and to the formation of the xanthylum cation by a two-photon process. In the presence of molecular oxygen, the radical is oxidized to the carbocation, but only when the counterion is Li^+ , Na^+ , or K^+ . No oxygen induced carbocation formation is observed in RbY or CsY. These results clearly demonstrate that even simple alkali metal cations can have a dramatic effect on oxidation reactions of organic radicals in zeolites.

Experimental Section

Materials. Xanthene-9-carboxylic acid (Aldrich) was used as received. NaY (Aldrich, LZ52 molecular sieves, Si/Al = 2.4) was first activated at 400 °C for 16 h to remove any absorbed water. Xanthene-9-carboxylic acid was then incorporated by mixing 5 mg of the organic compound dissolved in 10 mL of CH_2Cl_2 (OmniSolv, BDH) and 200 mg of activated zeolite for 1 h. The suspension was centrifuged and the isolated zeolite washed with CH_2Cl_2 and dried under vacuum, 10^{-3} Torr. During the incorporation of the precursor into the zeolite framework the utmost care was taken to keep the zeolite sample dry. The procedure for incorporation of XCOOH into the other cation exchanged zeolites was identical to that for incorporation into NaY.

The co-incorporation of XCOOH and MV^{2+} was accomplished by initially preparing a NaY sample containing methyl viologen dication with water as the carrier solvent. The loading level was one MV^{2+} per 10 zeolite cavities. The sample was dried in a vacuum oven to ensure the removal of the coabsorbed water. After the sample was dried, XCOOH was incorporated into the MV^{2+} /zeolite composites in the same manner as described above.

The exchanged zeolites were prepared by stirring NaY with 1 M aqueous solutions of the corresponding chlorides ($LiCl$, KCl , $RbCl$,

(48) Yoon, K. B. *Chem. Rev.* **1993**, *93*, 321–339.

(49) Bartl, J.; Steenzen, S.; Mayr, H.; McClelland, R. A. *J. Am. Chem. Soc.* **1990**, *112*, 6918–6928.

and CsCl) at 80 °C for 1 h. The zeolites were then washed until no chlorides appeared in the washing water and dried under vacuum. This procedure was repeated three times and the zeolite was calcinated between washings. NaY has three types of exchangeable cations. The number of cations per unit cell of zeolite Y are 16 site I cations, 32 site II cations, and 8 site III cations. It is well established that only site II and III cations are accessible to guest molecules.⁵⁰ The percent exchange was found to be 47% for LiY, 97% for KY, 44% for RbY, and 47% for CsY. It is known that for the larger cations such as Rb⁺ and Cs⁺ only the accessible Na⁺ which occupy type II and type III sites can be readily exchanged.¹ Thus, the maximum cation exchange is ~70%. Values of ~50% exchange indicate that a small percentage of type II cations are not completely exchanged. The low percent exchange for the LiY sample used in this study is because hydrated Li⁺ also does not readily exchange the type I cations. A second sample of LiY was prepared from NH₄⁺ exchanged Y zeolite. In this case more Li⁺ were incorporated and the percent exchange was found to be 80%. Unfortunately, due to the presence of acid sites XCOOH was not stable upon incorporation into this sample of NH₄-LiY.

The amount of XCOOH incorporated into the zeolite was calculated from the difference between the initial amount of the XCOOH and the amount that was recovered in the combined solutions measured by UV absorption. The loading level was found to be about 1 XCOOH per 15 cavities.

Determination of the stability of the XCOOH upon incorporation into the cation exchanged zeolites was carried out by re-extracting the incorporated material. The organic components were extracted from the zeolite by using a continuous solid-liquid extracting apparatus with CH₂Cl₂ as the solvent. The organic matter was analyzed by ¹H NMR (300 MHz, Varian Gemini).

Steady-state irradiation was carried out with a photoreactor containing eight 254-nm lamps. Ground-state diffuse reflectance measurements of XCOOH/MY samples were obtained with a Shimadzu UV-2101 PC

scanning spectrophotometer. Kubelka-Munk equations F(R) were plotted as a function of wavelength. The IR spectra were obtained with a Perkin-Elmer 580 B IR spectrophotometer equipped with a data station.

Laser Flash Photolysis. Time-resolved diffuse reflectance experiments were carried out with a nanosecond laser system previously described.⁵¹ The excitation source was the fourth harmonic (266 nm, <20 mJ, <8 ns/pulse) from a Continuum NY61-10 YAG laser. For the two laser and the photoinduced electron-transfer experiments a Lambda Physik Compex 102 excimer laser with a XeCl gas mixture (308 nm, <100 mJ, <20 ns/pulse) was used as the second excitation source. The samples were contained in quartz cells constructed with 3 × 7 mm² tubing and were either evacuated under reduced pressure (10⁻³ Torr) or purged with oxygen for a minimum of 30 min prior to photolysis. The data analysis was based on the fraction of reflected light absorbed by the transient (reflectance change $\Delta J/J_0$) where J_0 is the reflectance intensity before excitation and ΔJ is the change in the reflectance after excitation.

Acknowledgment. We gratefully acknowledge the Natural Sciences and Engineering Research Council of Canada (NSERC) for financial support of this research through an equipment and operating grant (F.L.C). In addition, we would like to thank Dalhousie University for the generous support of our research program. M.L.C. is grateful to the Spanish D.G.I.C.Y.T. for a scholarship. F.L.C is the recipient of an NSERC WFA. F.L.C and N.P.S thank J. Pincock for many useful discussions.

JA971524A

(50) Ramamurthy, V.; Turro, N. J. *J. Incl. Phenom. Mol. Recog. Chem.* **1995**, *21*, 239–282.

(51) Cozens, F. L.; O'Neill, M.; Bogdanova, R.; Schepp, N. P. *J. Am. Chem. Soc.* **1997**, *119*, 10652–10659.